Use of In Situ Air Flow Measurements to Study Permeability in Cracked Clay Soils

Tony Wells[1]; Stephen Fityus[2]; and David W. Smith[3]

Abstract: The work describes in situ measurements of crack induced permeability as a function of depth, (down to ~1.75 m), in clay soils at two field sites, using the gas flow technique described in an earlier study. The gas flow response to applied pressure was found to exhibit a significant nonlinearity at all depths indicating non-Darcian flow despite the fact that the flow was likely to be well within the laminar flow regime. Application of three-dimensional finite-element models to describe the gas flow revealed that the nonlinearity is likely to be an intrinsic behavior related to the soil-gas flow interaction. The Forchheimer compressible flow equation successfully simulated the behavior at all depths. The viscous and inertial permeability parameters obtained from this analysis showed a wide range of values which were closely correlated to the pore-water content of the soil medium, clearly showing the influence of ped swelling on the contraction of macrovoid channels in the structured clay soil.

DOI: 10.1061/(ASCE)1090-0241(2007)133:12(1577)

CE Database subject headings: Soil permeability; Clays; Darcy's law; Finite element method; Measurement; Cracking.

Introduction

A simple, rapid technique has been presented by Wells et al. (2006) in which the saturated hydraulic conductivity of soil media with macroporosity can be estimated using in situ gas permeability measurements in conjunction with a three-dimensional finite-element model of the gas flow behavior. This approach makes it possible to gather large quantities of hydraulic conductivity data more rapidly and cheaply than using more conventional experimental approaches such as those employing permeameters or oedemeters (e.g., Head 1994; Holland et al. 2000). Measurement efficiency is an important consideration as most soils exhibit significant spatial variability in hydraulic conductivity on a small scale, so that typically a large number of data points are required to adequately characterize deposits of interest.

A number of studies have been undertaken to determine hydraulic conductivities of soils from gas flow measurements (Blackwell et al. 1990; Loll et al. 1999; Iversen et al. 2001). Recently the interpretation of the pressure-flow data generated in such studies has been improved by the inclusion of a "shape factor" (Liang et al. 1995) to characterize the flow path length of the gas through the soil (Iversen et al. 2004). In all of these studies, however, the permeability measurements have been restricted to near-surface soil layers, and the use of a "shape factor approach" has limited the application of the gas flow technique to soil media that are homogeneous with respect to porosity and permeability.

Gas flow permeability measurement techniques are particularly suited to sandy or structured soils where bulk water movement under gravity is dictated by the distribution of cracks (macropermeability). Here the focus is on structured cohesive soils that include desiccated soils, pedal soils (Fityus et al. 2004b), or uncracked cohesive soils with an interconnected macropore structure (such as bioturbated fine sediments). The cracks in desiccated soils often occur to significant depths, however, their size and spacing is a function of the distribution of moisture in the soil, which varies with proximity to the surface. Currently there are no simple recognized techniques to measure the density or permeability of such cracks as a function of depth (Fityus et al. 2004b).

Such soils may be considered to have a dual/multiple porosity behavior, allowing rapid fluid movement through cracks and fissures with simultaneous, slower fluid movement within the soil peds. In general, the flow within the intact regions of cohesive soils will be orders of magnitude smaller than the flow through macrovoids, and consequently measurements in these soils using the proposed technique will effectively measure only the macrovoid porosity. Gas flows require little time to establish pressure/flow equilibrium when applied to the soil and the low gas viscosity ensures rapid access to the clay cracks. If applied over short time periods the introduction of a gas stream into the cracked clay structure does not affect crack size and therefore avoids complications arising from changes in soil structure that can occur as result of the wetting of swelling clay soils (Blackwell et al. 1990). The nondestructive nature of this test ensures that the crack structure of the clay remains unchanged over the short term enabling multiple tests to be carried out in each area. It is therefore possible to carry out repeated tests at progressively greater depths at

[1]Research Fellow, The School of Engineering, The Univ. of Newcastle, Callaghan, Newcastle 2308, Australia (corresponding author). E-mail: Tony.Wells@newcastle.edu.au

[2]Associate Professor, The School of Engineering, The Univ. of Newcastle, Callaghan, Newcastle 2308, Australia. E-mail: stephen.fityus@newcastle.edu.au

[3]Professor, Dept. of Civil and Environmental Engineering, The Univ. of Melbourne, Victoria 3010, Australia. E-mail: david.smith@unimelb.edu.au

Note. Discussion open until May 1, 2008. Separate discussions must be submitted for individual papers. To extend the closing date by one month, a written request must be filed with the ASCE Managing Editor. The manuscript for this paper was submitted for review and possible publication on May 11, 2006; approved on March 25, 2007. This paper is part of the ***Journal of Geotechnical and Geoenvironmental Engineering***, Vol. 133, No. 12, December 1, 2007. ©ASCE, ISSN 1090-0241/2007/12-1577–1586/$25.00.

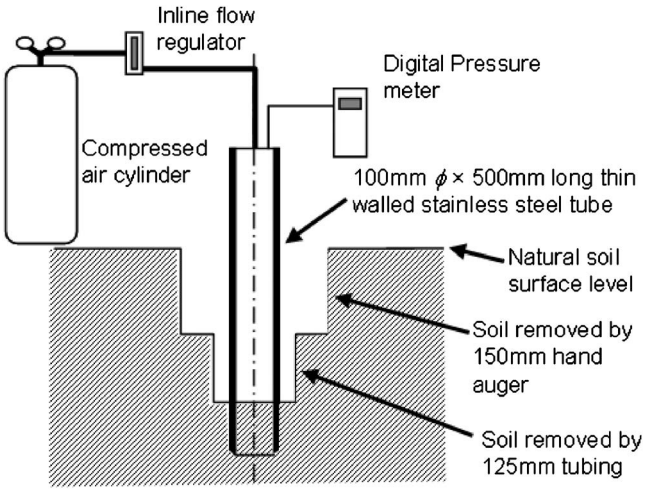

Fig. 1. Arrangement of field permeameter apparatus

a single location, thereby facilitating an estimation of the vertical variation in crack density.

The aim of this study is to extend the application of the air flow technique to include an examination of the permeability of structured clay soils to significant depths. The work describes in situ measurements of crack induced permeability as a function of depth in clay soils at two field sites using the gas flow technique described in Wells et al. (2006). Gas flow permeability measurements undertaken at depths well below the soil surface involve the gas flowing through soil layers of differing permeability as it permeates from the point of release to the soil surface. This scenario cannot be effectively modeled using the simple shape factor approach adopted in previous studies, (e.g., Iversen et al. 2004). In this study a three-dimensional finite-element flow model was employed to extend the application of the gas flow method to model gas flow through nonhomogeneous soil profiles from any release depth. As will become evident later in this paper the use of the finite-element model also allows for the inclusion of non-Darcy flow considerations into the flow model enabling an improved interpretation of the data obtained at the two field sites.

Methodology

In order to apply the previously developed experimental techniques to deep, natural profiles of cracked clay soil, it was necessary to adapt the technique to use at depth. As in the previous study (Wells et al. 2006), the air permeameter used in this study consisted of a 500-mm-long, 100-mm-diameter thin-walled delivery tube fabricated from a stainless steel tube, with a 3 mm beveled lower edge. To enable deployment down a drilled borehole the device was equipped with an adaptor for an extension handle.

The experimental arrangement employed is shown in Fig. 1. At the selected site, excess vegetation was first cleared and the 100-mm-diameter gas delivery tube pushed into the ground until the leading edge was embedded 50 mm below the natural ground level. Air at 200 kPa pressure from an air cylinder was fed through an inline flow regulator (40 L/min range) to the head of the tube at a variety of flow rates ranging from 1 to 35 L/min. Once a steady gas flow was achieved, the pressure in the headspace of the delivery tube was measured using a digital pressure meter (Comark C9551) which has a range of 0–15 kPa with a resolution of 1 Pa. Repeated measurements at different flow rates enabled a pressure versus flow (P-Q) curve to be generated.

To record the P-Q curve at the next depth (150 mm below the surface), a 150-mm-diameter hand auger was used to remove soil to a depth of 50 mm. A 125-mm-diameter stainless steel tube was then pushed 50 mm into the bottom of the augured hole. This tube was then extracted without rotation to remove a core of soil, leaving a broken soil surface at the base of the hole (now 100 mm deep), which was free of smearing. The 100-mm-diameter air delivery tube was then pushed a further 50 mm into the floor of the newly formed cavity (so that its bottom edge was 150 mm below the natural soil surface and a 50 mm deep plug of soil was contained in the delivery tube). Once in place, a new set of flow versus pressure data was generated. This process (auger, then soil core, then test) was repeated so that P-Q curves could be obtained at subsequent depths at 150 mm spacings, until the desired depth was reached, or until the macroporosity decreased to such an extent that the pressures generated forced the tube out of the ground.

Air permeameter field trial results were obtained at two sites, Maryland and Scone, located in the Hunter Valley region of New South Wales, on the eastern coast of Australia. Tests were conducted at five depths down to 1,200 mm at the Maryland site, and 11 depths down to 1,750 mm at the Scone site. The Maryland site is an existing research study site established in 1993 which has been used to obtain high quality data on moisture changes and soil movements in a residual clay profile for over a decade (Fityus et al. 2004a). The soil profile at the Maryland site consists of 250 mm of silty clay topsoil overlaying 900 mm of highly plastic residual clay which in turn overlays 600 mm of medium plastic clay showing relict rock structure (Fityus and Smith 2004). Below this lies highly weathered siltstone. Ground movements in the range of 47–75 mm due to climatic moisture changes have been recorded (Fityus et al. 2004a). Cracks at the soil surface during dry seasons up to 10 mm wide have also been observed. The Scone site is located approximately 150 km inland. The soil profile consists of 150 mm of slopewash colluvium topsoil, overlaying 500 mm of dark colored sandy clay with some gravels which in turn overlays 1,000 mm of paler gravely sandy clay. Clays on the Scone site commonly exhibit surface cracking widths in excess of 20 mm during dry summers. Some cracks as wide as these were evident at the time the results reported here were obtained. At the time of testing both sites were well drained. It was therefore assumed that no free water was present in the macrovoids ensuring that gas flow through the crack system was unimpeded by the presence of water in the larger voids.

Basic Numerical Model

The gas flow technique involves the delivery of gas at a range of pressures, (P), through the delivery tube at each depth and the measurement of the corresponding gas volumetric flowrate, (Q). The pressure-flow, (P-Q), relationship obtained at each depth is theoretically dominated by the intrinsic permeability of the soil at the tube exit and influenced to a lesser extent by the soil volume that the gas passes through as it permeates up to the soil surface (Wells et al. 2006). Wells et al. (2006) derived the governing equations for compressible gas flow through a granular medium, and demonstrated that the intrinsic permeability determined in this way could be used to estimate the saturated hydraulic conductivity. As a starting point for the present study, it was again assumed that Darcy's law, (Darcy 1856), adequately described the flow of gas through the macrovoid crack structure of the clay soils

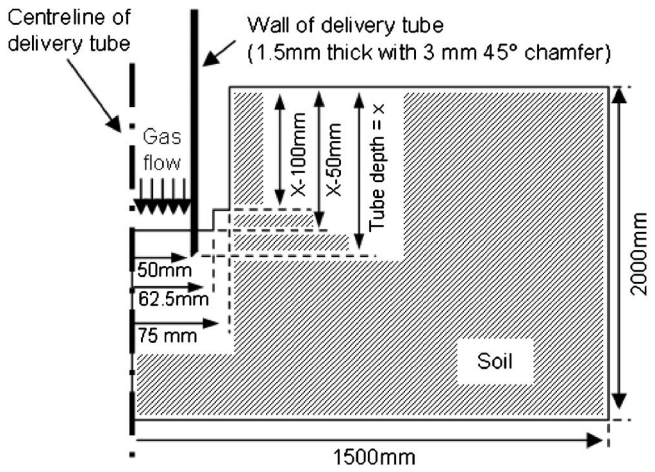

Fig. 2. Geometry employed in finite-element numerical model

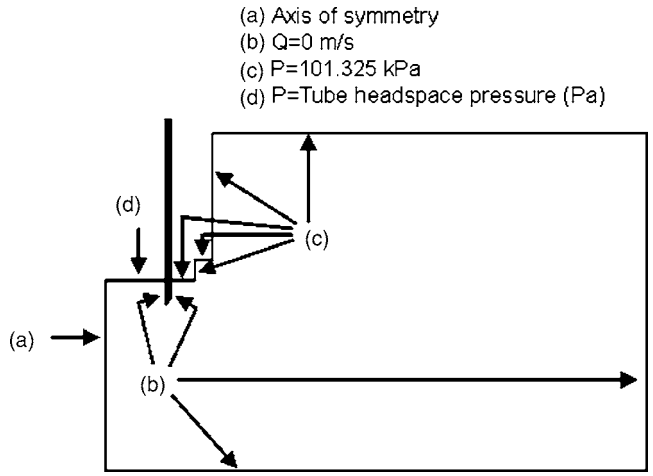

Fig. 3. Boundary conditions employed in finite-element model

$$Q = -k_g A \frac{\Delta h}{\Delta L} \tag{1}$$

In Eq. (1), $\Delta h/\Delta L$=hydrostatic head gradient; A=cross-sectional area through which the gas is flowing; and the proportionality constant k_g denotes the gas permeability of the porous medium. Incorporating the continuity equation for steady state compressible flow into Eq. (1) and rewriting in terms of intrinsic permeability yields the following description of Darcy gas flow through the macrovoid cracks

$$\nabla \cdot \left\{ -\frac{K_{\text{int}} M_g}{\mu RT} P \nabla P \right\} = 0 \tag{2}$$

In Eq. (2), K_{int}=intrinsic permeability of the medium; M_g=molecular weight of the gas (0.029 kg mol^{-1}); μ=gas dynamic viscosity (1.85×10^5 kg m^{-1} s^{-1}); R=universal gas constant (8.314 J K^{-1} mol^{-1}); T=absolute temperature; and P=gas pressure in the delivery tube headspace.

To determine the value of the intrinsic permeability that most accurately reproduces the P-Q relationships observed in the field, a numerical model of the testing arrangement was constructed within a three-dimensional (3D) axisymmetric finite-element framework using the FEMLAB software package. The geometry of the domain used in the finite-element model is illustrated in Fig. 2. The dimensions of the total soil volume domain (2 m deep with a radius of 1.5 m) were large enough to prevent significant gas flux through the bottom and outer radial surfaces of the soil volume. The choice of domain size was validated by comparing P-Q relationships predicted for this geometry with a one employing a far larger domain (5 m deep with a radius of 5 m). The difference between the pressure flow relationships predicted by the two models was less than 3%.

Boundary conditions employed in the finite-element model are illustrated in Fig. 3. Soil surfaces exposed to atmosphere (including those in the hole produced by the use of the 150 mm auger and 125 mm soil plug removal tube) were assumed to be at atmospheric pressure, while the soil surface intersected by the delivery tube (and through which the pressurized air may flow) was assumed to be at the headspace pressure recorded during the field trial. The gas flux was assumed to be negligible across the bottom and outer boundaries of the model space, as well as the line of symmetry. Within the soil domain Eq. (2) was used to describe the pressure-flow relationship. Approximately 45,000 Lagrange quadratic elements were used in the finite-element mesh.

To estimate the intrinsic permeability of the system at a given tube depth a value for K_{int} was assumed and the model prediction for the total gas flow determined by integrating the predicted gas flow across the soil surface

$$Q = -\frac{2\pi K_{\text{int}}}{\mu} \int_{r=0}^{r=a} r \frac{dP}{dz} dr \tag{3}$$

This procedure was repeated for the different gas pressures employed in the field producing a P-Q curve which was then compared to that obtained experimentally at the specified tube depth. A trial and error process utilizing differing values of K_{int} was then employed until the best match (as determined by maximizing the R^2 value) was obtained for a given depth between the predicted and observed P-Q curves.

One possible failing with this simple approach is that the calculations performed at each depth assume that the intrinsic permeability of the soil is uniform over the entire soil volume even though the optimized K_{int} values obtained from the P-Q data at different depths indicate otherwise. As the ultimate aim of this study is to examine the variation in permeability with depth a more complete model of the soil volume incorporating any changes in permeability with depth was also constructed. To a first approximation, this was achieved by subdividing the soil domain into a series of horizontal strata, each possessing a characteristic permeability, thereby allowing the permeability to vary in a piecewise way with depth. This approach is illustrated in Fig. 4 which shows the model used to simulate the 450-mm-deep Maryland field measurement.

Although this approach allows for a more realistic representation of soil profiles, it involves a greater degree of trial and error in the permeability determination for each layer which produces an optimum fit to the measured data. As a starting point each band was assigned an intrinsic permeability corresponding to that determined for the same depth in the preliminary numerical analysis. The pressure-flow relationship at each level was then reevaluated and compared with that observed experimentally, and where necessary, adjustments to the permeability of each layer were made.

Preliminary Results for Basic Model

Pressure-flow rate curves were obtained at five depths at the Maryland site (0–50, 150–200, 300–350, 400–450, and 600–

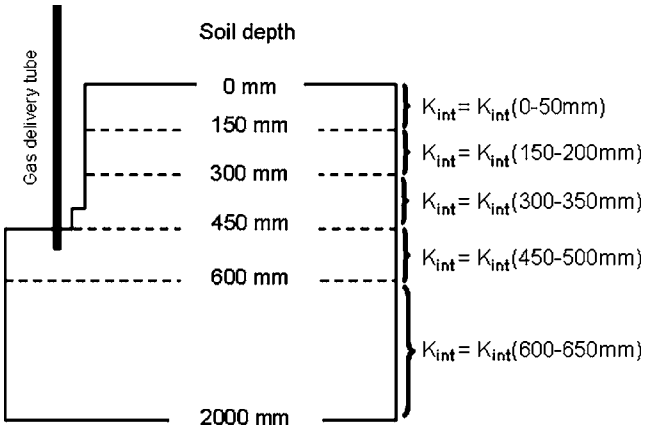

Fig. 4. Complete model geometry for Maryland field site model

650 mm) and 11 depths at the Scone site (0–50, 150–200, 300–350, 400–450, 600–650, 700–750, 850–900, 1,020–1,070, 1,180–1,230, 1,500–1,550, and 1,700–1,750 mm). Each depth was tested to a maximum of $P=15$ kPa or $Q=35$ L/min (whichever was reached first). The P-Q data obtained is shown in Figs. 5 and 6. In all cases the expected positive relationship between applied gas pressure and flow through the soil volume was evident, however there was a significant curvature clearly evident in all of the results which was not observed in the previous study involving granular soils (Wells et al. 2006). A cursory examination of the raw data also indicated that each of the test sites was characterized by a large range of permeabilities, which were a complex function of depth [for example, note the relatively high permeability observed at 700–750 mm at the Scone site, (Fig. 6)]. The Scone data exhibited two discrete bands of behavior; one grouping of highly permeable layers (0–50, 150–200, 400–450, 600–650, 700–750, and 850–900 mm) and one group of considerably less permeable layers observed principally at greater depths (1,020–1,070, 1,180–1,230, 1,700–1,750, and 300–350 mm). The permeability observed at the Maryland site on the whole fitted between the two extremes observed for the Scone site.

As a result of the nonlinear nature of the P-Q relationship numerical analysis of the data using the basic compressible form of the Darcy equation [Eq. (2)] was deemed to be unsatisfactory. Fig. 7, which shows the fit to the 0–50 mm data obtained at the Maryland site, demonstrates that the basic model is only capable of predicting linear P-Q relationships, and that these are a poor approximation of the trends observed in this study. The 0–50 mm Maryland pressure-flow curve, for example, can be characterized by intrinsic Darcian permeabilities ranging from a low of 5.94×10^{-11} m^2 up to a maximum value of 1.06×10^{-10} m^2. In an attempt to better explain and model the observed nonlinear behavior, more advanced versions of the constitutive equation describing the flux were developed.

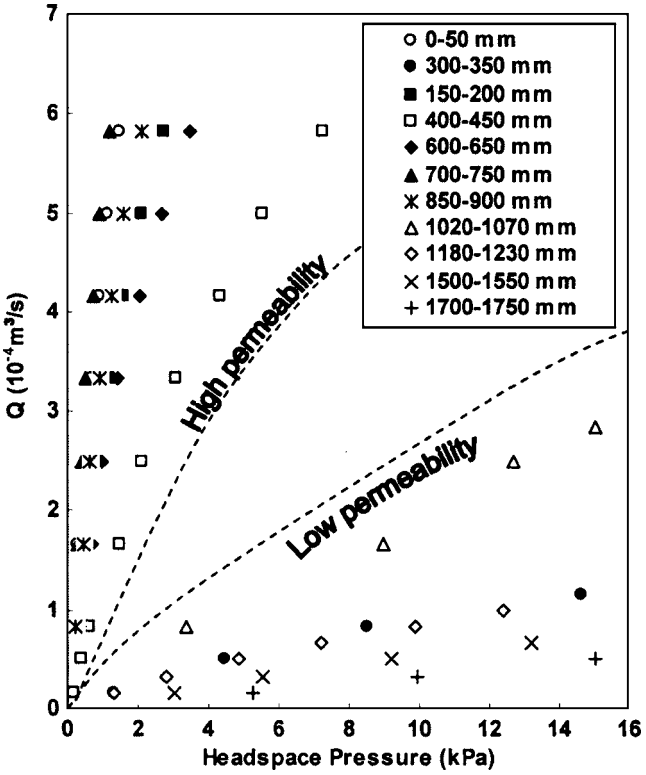

Fig. 6. Pressure flow curves observed at differing depths at Scone field site

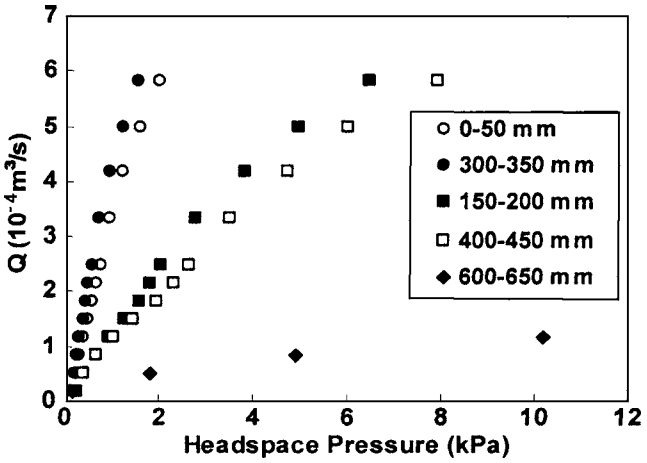

Fig. 5. Pressure flow curves observed at differing depths at Maryland field site

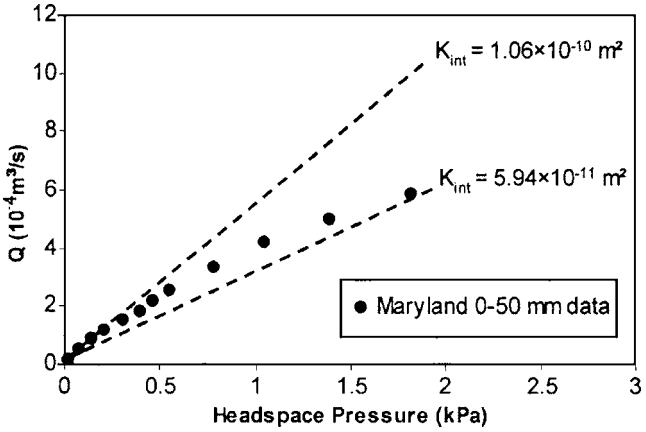

Fig. 7. Nonlinear behavior observed for 0–50 mm pressure flow curve—Maryland site

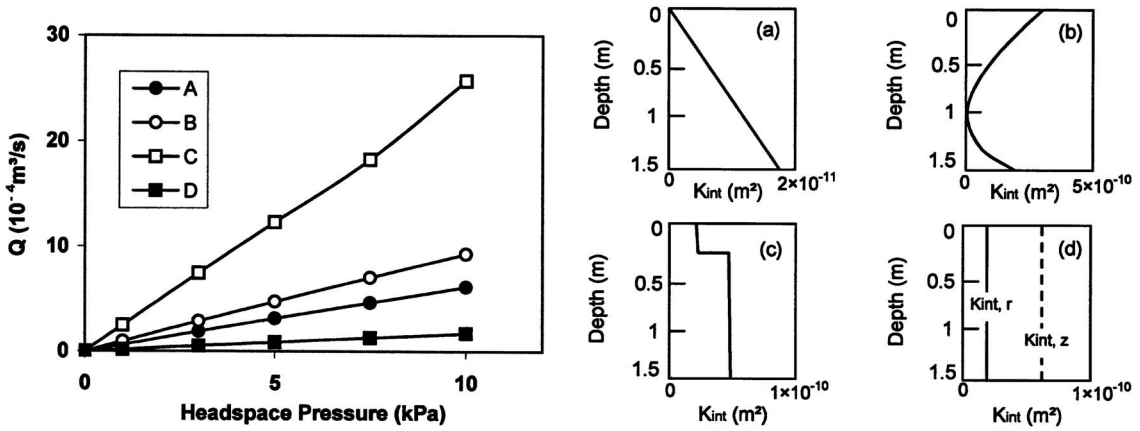

Fig. 8. Effect of different intrinsic permeability scenarios on linearity of pressure flow relationship (assuming compressible Darcy flow): (A) linear change in K_{int}; (B) nonlinear change in K_{int}; (C) step change in K_{int}; (D) $K_{int,r} \neq K_{int,z}$

Advanced Numerical Models

Two possibilities which could account for the highly nonlinear experimental pressure-flow data were identified and explored. The first assumes that the variations in permeability within each layer are more complicated than originally assumed and that these are causing the nonlinear behavior observed in the results. The second possibility assumes the presence of second-order phenomena that is not accounted for in the basic compressible Darcy flow model.

Nonuniform Intrinsic Permeabilities within Individual Soil Layers

P-Q curves were generated for a number of permeability scenarios using the existing 3D axisymmetric finite-element model for 450 mm tube depth and retaining the compressible Darcy flow model [Eq. (2)] detailed above. The results are presented in Fig. 8. The scenarios considered, included linear changes in K_{int} with depth (distribution A in Fig. 8), nonlinear changes in K_{int} with depth (distribution B in Fig. 8), step changes in K_{int} (distribution C in Fig. 8), and anisotropic K_{int} behavior ($K_{int,r}$ in the radial or horizontal direction does not equal $K_{int,z}$ in the vertical direction: [distribution (D) in Fig. 8]. As illustrated in Fig. 8, all of these hypothetical variations produced linear *P-Q* relationships, indicating that permeability variations cannot produce the distinct curvature in the *P-Q* measurements that is evident in the results obtained at the two field sites.

Gas Slippage at Air/Soil Interface

At low pressures "slippage" of gas molecules at the air/soil interface is sometimes observed which produces higher than expected gas flow rates for a given pressure gradient (Klinkenberg 1941). In such cases Klinkenberg proposed the following relationship between the gas permeability and mean pressure

$$k_g = k_L + C\left[\frac{1}{P_{av}}\right] \tag{4}$$

The pressure-flow data obtained in the field trials, however, shows a slowdown in gas flow (relative to the predicted Darcy value) as pressure increases—the opposite of that predicted by the Klinkenberg effect. Furthermore, the relationship suggested in Eq. (4) does not appear to be valid for the measured data, as a plot of the gas permeability constant against the reciprocal of the average pressure (here assumed to be the average of the tube head pressure and atmospheric pressure—Fig. 9) does not produce the linear relationship predicted by Eq. (4).

Inclusion of Non-Darcy Flow Effects

Darcy's law is derived from experiments conducted at low velocities and considers only the viscous effects in formulating the relationship between pressure gradients and laminar fluid flow. Deviations from Darcian behavior might be expected in laminar/turbulent transitional or purely turbulent flow regimes which are characterized by the presence of vortices and chaotic flow. To determine the flow conditions under which the gas permeability tests took place it was assumed that the flow behavior within the clay cracks was analogous to flow between parallel plates and hence the Reynolds number was calculated as follows

$$R_p = \frac{\rho U D_h}{\mu} \tag{5}$$

In Eq. (5) R_p=plate flow Reynolds number; ρ=density of air (kg/m^3); U=air velocity (m/s); and D_h=hydraulic diameter (m) which for flow between parallel surfaces is defined as equal to twice the crack width. Previous studies of the Maryland site (Moe

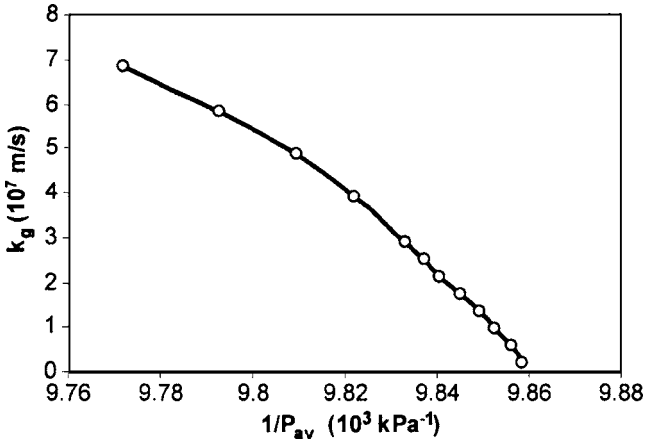

Fig. 9. Variation of air permeability with reciprocal of average pressure for Maryland 0–50 mm field data

et al. 2003) indicate that median crack widths are of the order of 3 mm and fall roughly onto a 50×50 mm grid. Using these values to calculate the flow area and hydraulic diameter, the Reynolds numbers for the flow experiments presented in this study fall in the range of approximately 6 (low pressures/flows) to 230 (at high pressures/gas flowrates). These values are well below the estimated laminar-turbulent transition region of $R_p = 2{,}300$ (Hanks 1963), suggesting that the deviations from Darcy's law took place well within the laminar flow region.

Deviations from Darcy's law have been observed previously in laminar flow through ceramic foams (Innocentini et al. 1999, 2000; Richardson et al. 2000), fluid flow in nonuniform capillary tubing (Dullien and Azzam 1973), and in cases where molecular forces or electrochemical reactions are present (Bennethum and Giorgi 1997). To our knowledge this is the first time such behavior has been observed in gas flow through cracked soil media. Recently numerical simulations of Navier–Stokes flow in two-dimensional porous media (Andrade et al. 1999; Costa et al. 1999) have shown that departures from Darcy's law in flow through a high porosity percolation structure can be explained in terms of an inertial contribution to the laminar flow of fluid through the void space. The additional inertial effects serve to slow down flow for a given pressure differential—a phenomenon that is consistent with the observations of this study.

The classical approach to characterizing the macroscopic effect of inertia on flow through a porous media is through the use of the Forchheimer equation (Forchheimer 1914)

$$\frac{\mu}{k_1} U + \frac{\rho}{k_2} U^2 = -\nabla P \tag{6}$$

From Eq. (6), the fluid velocity can be written as the following function of pressure, density, and viscosity

$$U = -\frac{k_2 \mu}{2\rho k_1} + \frac{k_2}{2\rho} \sqrt{\frac{\mu^2}{k_1^2} - \frac{4\rho}{k_2} \nabla P} \tag{7}$$

Combining the above expression with the continuity equation for steady-state compressible flow

$$\nabla \cdot \{\rho U\} = 0 \tag{8}$$

produces the following model which can be used to describe the non-Darcian fluid flow within the finite-element domain

$$\nabla \cdot \left\{ -\frac{k_2 \mu}{2k_1} + \frac{k_2}{2} \sqrt{\frac{\mu^2}{k_1^2} - \frac{4\rho}{k_2} \nabla P} \right\} = 0 \tag{9}$$

Fitting Eq. (9) to the field data was accomplished in a similar fashion to that previously described for the Darcy's law model using a 3D finite-element model that retains the domain boundary conditions detailed earlier. In this case, however, two parameters, (k_1 and k_2), had to be optimized for the pressure-flow curve recorded at each site and depth. A trial and error approach was employed and what might have been a time consuming process was significantly shortened by first making the following approximation of Eq. (6)

$$\frac{\mu}{k_1} U_{\text{th}} + \frac{\rho}{k_2} U_{\text{th}}^2 = -\frac{(P - P_{\text{atm}})}{L} \tag{10}$$

In Eq. (10), U_{th}=gas velocity in the tube headspace; and L=pseudoequivalent path length through the soil over which the pressure gradient dissipates. With a knowledge of the viscosity and average gas density at the field conditions good initial estimates for the parameters k_1 and k_2 were obtained by solving Eq. (10) using a pseudoequivalent path length of 0.07 m. Fully optimized values for the two permeability coefficients were then obtained from a (greatly shortened) trial and error process.

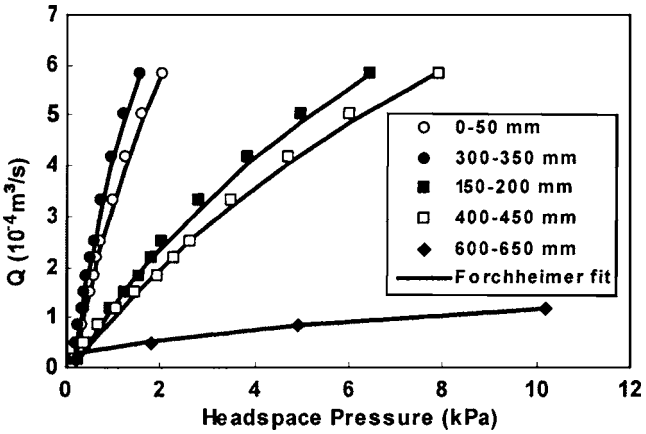

Fig. 10. Forchheimer fit to Maryland field pressure flow data

The final fit of the compressible flow, Forchheimer-based finite-element flow model to the field data is shown in Figs. 10 and 11. The Forchheimer model was able to successfully fit the *P-Q* data at each depth tested at the two field sites, with R^2 values >0.99 in the majority of cases. The Forchheimer model fit to the nonlinear *P-Q* data was far superior to that obtained when using the Darcy law model (compare for instance the fit to data in Figs. 10 and 11 with the fit to the data in Fig. 7). Table 1 lists the best fit Darcian (k_1) and non-Darcian (k_2) values obtained at the different depths. The variation in the k_1 and k_2 values obtained at the different depths was approximately 1–2 orders of magnitude, indicating that there was a considerable variation in cracked soil permeability across the range of depths examined. For both sites

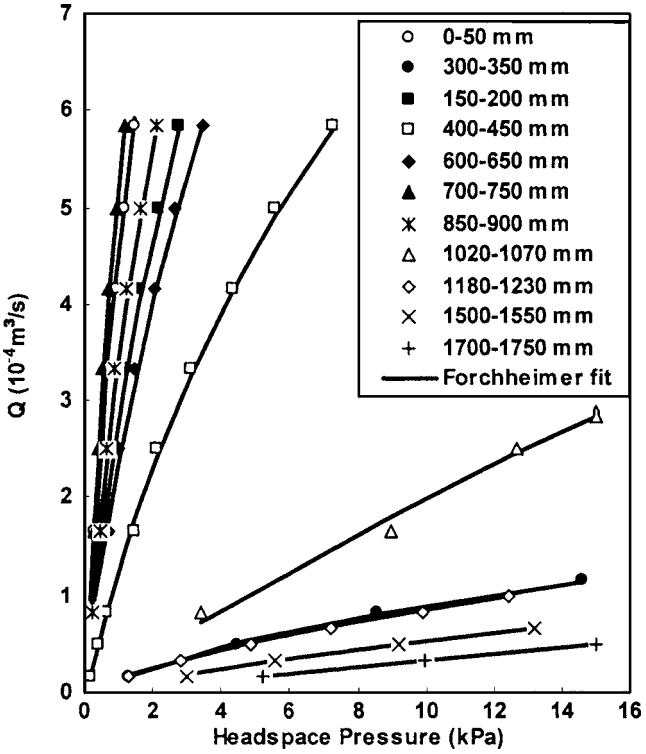

Fig. 11. Forchheimer fit to Scone field pressure flow data

Table 1. Permeability Constants Obtained at Two Field Sites Using Forchheimer's Equation

Site	Depth (10^{-3} m)	k_1 (10^{-10} m^2)	$-k_2$ (10^{-7} m)
Scone			
	0–50	2.59	5.35
	150–200	0.73	3.14
	300–350	0.03	0.02
	450–500	0.32	1.21
	600–650	0.56	2.76
	700–750	1.93	7.07
	850–900	0.99	4.31
	1,020–1,070	0.04	0.69
	1,180–1,230	0.02	0.03
	1,500–1,550	0.02	0.02
	1,700–1,750	0.01	0.07
Maryland			
	0–50	1.13	5.24
	150–200	0.32	1.53
	300–350	1.68	5.61
	450–500	0.25	1.42
	600–650	0.13	0.02

the absolute value of the ratio of non-Darcian to Darcian permeability parameter (k_2/k_1) ranged from 150 to 15,000 m. Such results are in agreement with analogous studies undertaken with ceramic foams (Innocentini et al. 1999, 2000) where k_2/k_1 ratios of 20–33,000 m were observed.

Discussion of Results

At all depths the field data revealed a distinct and consistent nonlinearity in the relationship between the applied pressure and the resulting gas flowrate (Figs. 10 and 11). Curvature observed in the results of near surface (0–50 mm) tests, as well as the findings of numerous finite-element simulations, all point to the conclusion that this phenomenon is not linked to nonuniformity in soil permeability, nor is it a function of the testing depth. Rather, the nonlinear *P-Q* response is an inherent property of the gas-soil flow interaction in these cracked clay soils. It is apparent from the early onset of curvature, that even at low gas flowrates, Darcy's law does not adequately characterize the gas flow behavior. It is also clear, at least in the case of clay soils at the two sites examined in this study, that to fully characterize the permeability of the clay soil at any depth, a range of *P-Q* values must be obtained. Evaluation of permeability using a single *P* versus *Q* datum, while potentially convenient if many sites are to be tested, will lead to erroneous permeability estimates in soils such as these in which Darcy's law is not applicable. This finding differs from that observed for the case of measurements undertaken in granular soils (Wells et al. 2006), where the *P-Q* relationship can be estimated by a single datum, as it is well approximated by a linear trend at all flow rates and pressures.

Processing of the field data using the compressible-flow Forchheimer finite-element model yielded a wide range of Darcian (viscous) and non-Darcian (inertial) permeability constants which appear to be a complex function of depth. Plotting the two parameters as a function of depth at the two sites (Fig. 12) reveals that the two permeability constants follow similar trends with depth, and that the variation in the two parameters appears to be closely linked to the soil conditions at the depth of measurement. In back-calculating the Forchheimer parameters, it was found that the values ascribed to a particular layer (at the mouth of the tube) are relatively insensitive to the values ascribed to adjacent layers in the profile.

This is especially the case for the Scone site [Fig. 12(a)] where a distinct minimum permeability is observed in the black clay layer lying immediately below the surface soil layer. This is followed at increasing depth by a sharp increase in permeability at the junction between black and brown clay horizons, after which the permeability again decreases with increasing depth.

The shifts in permeability with depth reflect changes in the soil structure (i.e., crack size/density) throughout the profile. They may be due to different expansive potential in the soil layers at different depths, or to differences in the soil water held at different levels in the soil. In general, for a particular soil type, it is expected that soils at higher water contents are less cracked, and so their macrovoid permeability should be lower. To consider the Forchheimer parameter variations further, the gravimetric water contents of the soils extracted during the excavation process are compared with the permeability constants determined for each tested depth.

Fig. 13 shows the relationship between the inverse of the permeability constants and the water content of the clay soils, as a function of depth for both sites. The data indicate a close relationship between the resistance to flow (as represented by $1/k_1$ and $1/k_2$) and the clay soil water content, as expected; that is, higher

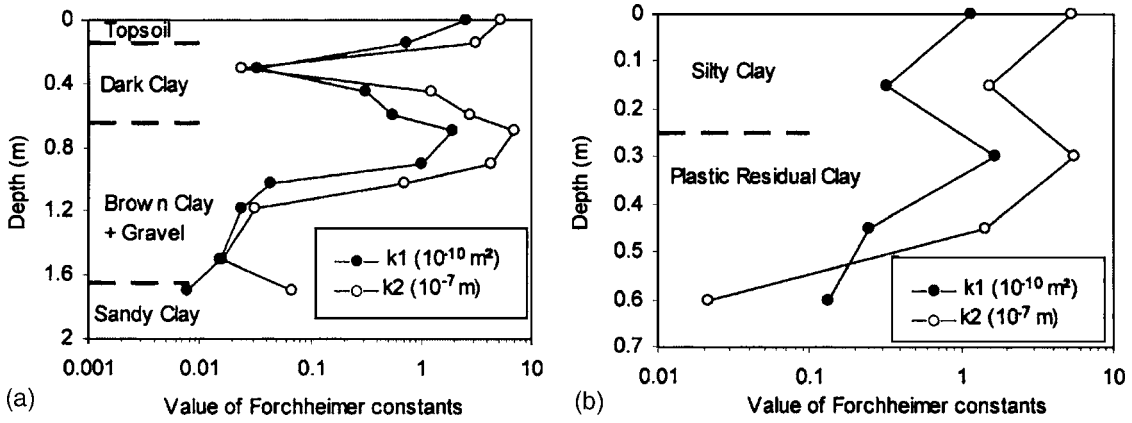

Fig. 12. Variation of permeability constants k_1 and k_2 with depth at: (a) Scone; (b) Maryland

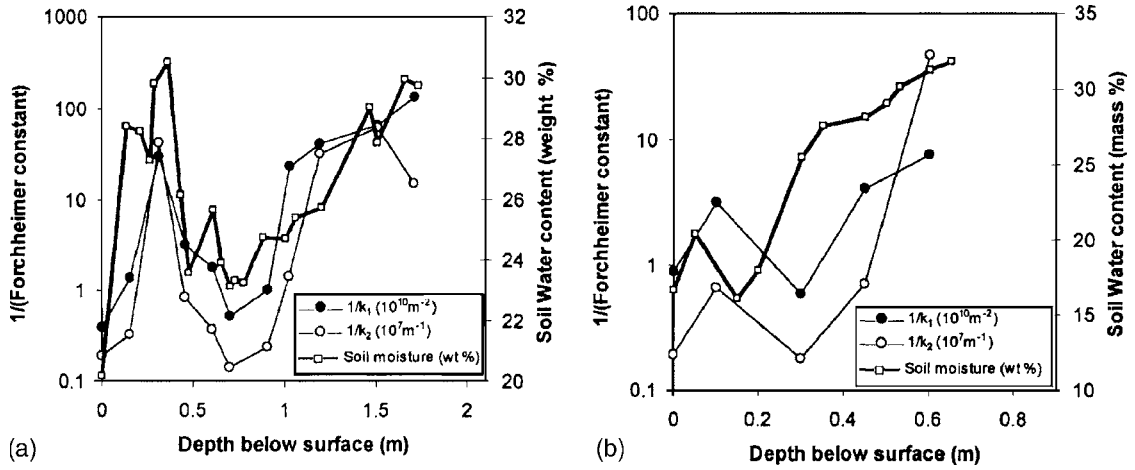

Fig. 13. Correlation between soil water content and inverse of Forchheimer constants for: (a) Scone; (b) Maryland site

permeability values coincide with lower water contents and vice versa. The correlation is particularly good for the Scone site [Fig. 13(a)].

The results of Table 1 and Fig. 13(a) in particular, give an insight into the complex behavior of cracking soil profiles. The higher water content/low permeability values between 250 and 450 mm are likely to represent the remnants of a wetting front, which could only propagate to a shallow depth before a continuation of drying conditions at the surface produced a drying front immediately above it. The high soil moisture levels at the wetting front resulted in the lower permeability observed at 350 mm depth at the Scone site. The low water content and higher permeability at 700–750 mm correspond to the dry soil beyond the wetting front.

Applicability and Significance

In considering the aims and outcomes of this research, it is necessary to appreciate the context of the problem being considered. Moisture flow in a cracked, heavy clay is a very complex phenomenon, involving simultaneous processes of moisture flow at different scales in a highly structured, deforming medium. Processes include the bulk (gravitational) flow of water through interaggregate/interpedal spaces (cracks and macrovoids), capillary flow of water through interparticle (intraaggregate) spaces, and diffusion of water into and out of intraparticle spaces. When bulk water is applied to the surface of a cracked soil, the response is dynamic, initially dominated by rapid inflow under gravity, and then by dispersal of this water by capillary flow and diffusion. For a given amount of water in the cracked soil profile, there is a tendency for bulk/free water to be rapidly and totally adsorbed/absorbed into soil aggregates and particles, leaving the macrovoid/crack network superficially dry. Hence, under typical conditions, the macrovoid network does not contain free water. Hence, as long as air permeability is not measured directly after rainfall, it will not be affected by water in the macrovoids.

To the writers' knowledge, the dynamics of wetting and drying in a cracked clay soil has not yet been rigorously modeled in a fully coupled way, accounting for the hierarchy of different pore and particle structures and moisture flow at all scales. Because of the differences in the rates of moisture movement at different scales, a logical simplification to make this problem more tractable, is to model the infiltration as a multistage process: first, allowing bulk water to rapidly permeate the cracked soil, and then, allowing the water in the cracks to disperse and diffuse within the soil elements. In the writers' experience, bulk water can flow into a cracked clay soil almost as fast as rainfall can deliver it; free water in cracks is taken up by soil elements in a matter of 1 or 2 days; but adsorbed/absorbed water can take weeks or months to redistribute.

This research provides a method by which the permeability of a cracked soil to bulk water can be determined. This allows the primary and most rapid process, of getting water into a cracked soil, to be modeled. The response of the cracked soil to the water in the cracks, and its subsequent redistribution within the soil, is a bigger issue, and is not considered here. The example presented above demonstrates how the permeability of a cracked clay soil profile can vary over two orders of magnitude over a relatively short distance, and how the response of a cracked clay soil profile to heavy rainfall, irrigation, or a flood event may be seriously affected by its antecedent moisture condition. This potentially common situation would be difficult to characterize using conventional field or laboratory measurement techniques. Clearly, the work detailed in this paper represents a snapshot of the permeability profile of each site at a given set of soil moisture conditions. It cannot, and it is not intended to, fully describe the wetting of the entire soil profile.

One issue that arises with the proposed methodology of using air permeability to determine hydraulic conductivity is the possible effect of encapsulated air on the inferred hydraulic conductivity. Theoretically, air will not be trapped by water films in a soil permeated by air, but it may be trapped in a soil permeated by water. If this occurred to a significant extent, the immobile air would effectively reduce the porosity, and hence permeability of the cracked soil. This means that the hydraulic conductivity estimated using air flow would be an overestimate of the true value. It is considered, however, that any encapsulated will be largely restricted to smaller pores in the interior of soil elements (peds) and so does nothing to affect the permeability of the interconnected macrovoids. As the cracks are mostly significantly larger than the intergranular pores, significant air is unlikely to be entrained in the interconnected crack network by water films.

Future work will expand on the current study by examining the same sites under a range of moisture conditions and use this information to build up a picture of permeability changes with time over a range of soil suction conditions as wetting fronts move up and down the soil profile. We believe that the gas flow

method, which enables the permeability profile to be determined without itself significantly altering the soil structure, is an ideal tool to study such phenomena in expansive clay soils.

Future studies will also seek to determine the nature of the relationship between the gas flow and water flow through cracked clay soils. Previous work by the authors (Wells et al. 2006) showed that the gas permeability, k_g, can be used to calculate the intrinsic permeability, K_{int}, and hence estimate the saturated hydraulic conductivity of granular soils for Darcian flow conditions. This study indicates that the situation for flow through cracked clay soils, which includes inertial effects, is more complicated. Future work will seek to address the following questions: (1) is water flow through cracked clay soils influenced by inertial factors in the same fashion as gas flows? (2) Can the Forchheimer parameters obtained from gas flow experiments be directly related to the relevant water flow permeability properties?

Conclusions

This study successfully demonstrates the use of the gas flow technique to estimate the permeability of the macrovoid system in cracked clay soils in the field. The gas flow response to applied pressure was found to exhibit a significant nonlinearity at all depths indicating non-Darcian flow despite the fact that the flow was likely to be well within the laminar flow regime. As a result the gas flow rate response to a range of applied pressure must be obtained at each sampling point if the permeability behavior of the clay at a particular depth is to be fully characterized. Application of 3D finite-element models to describe the gas flow revealed that the nonlinearity was not the result of spatially nonuniform permeability but it is likely to be an intrinsic behavior related to the soil-gas flow interaction. The inclusion of a non-Darcian (Forchheimer) compressible flow equation into the finite-element model resulted in a satisfactory simulation of the flow behavior at all depths. The viscous and inertial permeability parameters obtained from this analysis showed a wide range of values which were closely correlated to the pore-water content of the soil medium, clearly showing the influence of ped swelling on the contraction of macrovoid channels in the structured clay soil.

Acknowledgments

The writers wish to acknowledge the contribution of Mr. Hlwan Moe in the development of the basic air-flow technique and for his assistance in carrying out the fieldwork. This research has been carried out with the financial support from the Australian Research Council (ARC). The numerical modeling was undertaken using FEMLAB version 2.1 (Comsol Inc., United States).

Notation

The following symbols are used in this paper:

A = cross-sectional area through which gas flows (m^2);
D_h = hydraulic diameter used in calculating plate Reynolds number (=2×crack width for flow between parallel surfaces) (m);
K_{int} = intrinsic permeability of porous medium (m^2);
k_g = gas permeability of porous medium ($m\ s^{-1}$);
k_L = liquid permeability of porous medium ($m\ s^{-1}$);
k_1 = viscous (Darcian) Forchheimer permeability constant (m^2);
k_2 = inertial Forchheimer permeability constant (m);
L = pseudoequivalent path length through which gas pressure dissipates (m);
M_g = molecular weight of gas (in this study air was used=0.029 $kg\ mol^{-1}$);
P = pressure in gas delivery tube headspace (kPa);
P_{av} = average gas pressure in soil [=$(P+101.325)/2$] (kPa);
Q = volumetric flowrate of gas ($m^3\ s^{-1}$);
R = universal gas constant (8.314 $J\ K^{-1}\ mol^{-1}$);
R_p = plate Reynolds number (-);
r = radial distance from center of gas delivery tube (m);
T = absolute temperature (K);
U = gas velocity ($m\ s^{-1}$);
U_{th} = gas velocity in gas delivery tube headspace ($m\ s^{-1}$);
$\Delta h/\Delta L$ = hydrostatic pressure gradient (-);
μ = dynamic viscosity of air ($1.85\times10^{-5}\ kg\ m^{-1}\ s^{-1}$); and
ρ = density of air ($kg\ m^{-3}$).

References

Andrade, J. S., Jr., Costa, U. M. S., Almeida, M. P., Makse, H. A., and Stanley, H. E. (1999). "Inertial effects on fluid flow through disordered porous media." *Phys. Rev. Lett.*, 82(6), 5249–5252.

Bennethum, L. S., and Giorgi, T. (1997). "Generalized Forchheimer equation for two-phase flow based on hybrid mixture theory." *Transp. Porous Media*, 26(3), 261–275.

Blackwell, P. S., Ringrose-Voase, A. J., Jayawardane, N. S., Olsson, K. A., McKenzie, D. C., and Mason, W. K. (1990). "The use of air-filled porosity and intrinsic permeability to air to characterize structure of macropore space and saturated hydraulic conductivity of clay soils." *J. Soil Sci.*, 41, 215–228.

Costa, U. M. S., Andrade, Jr., J. S., Makse, H. A., and Stanley, H. E. (1999). "The role of inertia on fluid flow through disordered porous media." *Physica A*, 266(1–4), 420–424.

Darcy, H. (1856). "Les fountaines publique de la Ville de Dijon." *Dynamics of fluids in porous media*, Bear, J., ed., Elsevier, New York.

Dullien, F. A. L., and Azzam, M. I. S. (1973). "Flow rate-pressure gradient measurements in periodically non-uniform capillary tubes." *AIChE J.*, 19(2), 222–229.

Fityus, S. G., and Smith, D. W. (2004). "The development of a residual soil profile from a mudstone in a temperate climate." *Eng. Geol. (Amsterdam)*, 74, 39–56.

Fityus, S. G., Smith, D. W., and Allman, M. A. (2004a). "Expansive soil test site near Newcastle." *J. Geotech. Geoenviron. Eng.*, 130(7), 686–695.

Fityus, S. G., Smith, D. W., Imre, E., and Rajkai, K. (2004b). "Model framework for structure and volume changes in cracking expansive clay soils." *Proc., 9th ANZ Geomechanics Conf.*, Auckland, New Zealand, 598–604.

Forchheimer, P. (1914). *Hydrolik*, Tuebner, Leipzig, Berlin, 116–118.

Hanks, R. W. (1963). "The laminar-turbulent transition for flow in pipes, concentric annuli, and parallel plates." *AIChE J.*, 9(1), 45–48.

Head, K. H. (1994). *Manual of soil laboratory testing, permeability, shear strength and compressibility tests*, Vol. 2, Pentech Press, London.

Holland, D. F., Yitayew, M., and Warrick, A. W. (2000). "Measurement of subsurface unsaturated hydraulic conductivity." *J. Irrig. Drain. Eng.*, 126(1), 21–27.

Innocentini, M. D. M., Pardo, A. R. F., and Pandolfelli, V. C. (2000). "Influence of air compressibility on the permeability evaluation of refractory castables." *J. Am. Ceram. Soc.*, 83(6), 1536–1538.

Innocentini, M. D. M., Pardo, A. R. F., Salvini, V. R., and Pandolfelli, V. C. (1999). "How accurate is Darcy's Law for refractories." *Am. Ceram. Soc. Bull.*, 78(11), 64–68.

Iversen, B. V., Moldrup, P., and Loll, P. (2004). "Runoff modelling at two field slopes: use of *in situ* measurements of air permeability to characterize spatial variability of saturated hydraulic conductivity." *Hydrolog. Process.*, 18, 1009–1026.

Iversen, B. V., Schjønning, P., Poulsen, T. G., and Moldrup, P. (2001). "*In situ*, on-site and laboratory measurements of soil air permeability: Boundary conditions and measurement scale." *Soil Sci.*, 166(2), 97–106.

Klinkenberg, L. J. (1941). *The permeability of porous media to liquid and gases*, American Petroleum Institute, New York.

Liang, P., Bowers, C. G., Jr., and Bowen, H. D. (1995). "Finite element model to determine the shape factor for soil air permeability measurements." *Trans. ASAE*, 38(4), 997–1003.

Loll, P., Moldrup, P., Schjønning, P., and Riley, H. (1999). "Predicting saturated hydraulic conductivity from air permeability: Application in stochastic water infiltration modeling." *Water Resour. Res.*, 35(8), 2387–2400.

Moe, H., Fityus, S. G., and Smith, D. W. (2003). "Study of a cracking network in residual expansive clay." *Proc., 2nd Asian Conf. on Unsaturated Soils (Unsat Asia 2003)*, Osaka, Japan, 149–154.

Richardson, J. T., Peng, Y., and Remue, D. (2000). "Properties of ceramic foam catalyst supports: Pressure drop." *Appl. Catal., A*, General 204, 19–32.

Wells, T., Fityus, S., Smith, D. W., and Moe, H. (2006). "The indirect estimation of hydraulic conductivity of soils using measurements of gas permeability. I: Laboratory testing with dry granular soils." *Australian J. Soil Research*, 44, 719–725.